International Journal of Heat and Mass Transfer 52 (2009) 4254–4263

Contents lists available at ScienceDirect

International Journal of Heat and Mass Transfer

journal homepage: www.elsevier.com/locate/ijhmt

On the onset of natural convection in differentially heated shallow fluid layers with internal heat generation

George K. Perekattu, C. Balaji *

Heat Transfer and Thermal Power Laboratory, Department of Mechanical Engineering, Indian Institute of Technology Madras, Chennai 600 036, India

ARTICLE INFO

Article history:
Received 11 June 2008
Received in revised form 1 January 2009
Accepted 3 April 2009
Available online 1 June 2009

Keywords:
Rayleigh Benard convection
Internal heat generation
Linear stability analysis
Stability curves
Critical Rayleigh number
Numerical investigation

ABSTRACT

This paper reports the results of an analytical and numerical investigation to determine the effect of internal heat generation on the onset of convection, in a differentially heated shallow fluid layer. The case with the bottom plate at a temperature higher than the top plate mimics the classical Rayleigh Benard convection. However, internal heat generation adds a new dimension to the problem. Linear stability analysis is first carried out for the case of an infinitely wide cavity. The effect of aspect ratio on the onset of convection is studied by solving the full Navier–Stokes equations and the equation of energy and observing the temperature contours. A bisection algorithm is used for an accurate prediction of the onset. The numerical results are used to plot the stability curves for eight different aspect ratios. A general correlation is developed to determine the onset of convection in a differentially heated cavity for various aspect ratios. For an aspect ratio of 10, it is seen that the cavity approaches the limit of an infinite cavity. Analytical results obtained by using linear stability analysis agree very well with the "full" CFD simulations, for the above aspect ratio.

1. Introduction

Natural convection in a shallow horizontal fluid layer with internal heat generation is gaining immense interest in contemporary heat transfer research, as it has a number of applications related to atmospheric sciences, as for example, in convection from the earth's mantle, convection in the outer layer of sun and stars, as discussed below. The convection in the earth's atmosphere can be modeled using the Rayleigh Benard convection as the temperature of the lower layers is higher than that of the upper layers. The heat transfer from the clouds and the associated phase change due to the condensation/evaporation of water vapor/liquid water and melting/freezing of ice/liquid water can be modeled using internal heat generation. The Meso scale Cellular Convection (MCC) is usually considered as an atmospheric manifestation of Rayleigh Benard convection (Agee et al. [1], Rothermel and Agee [2]). The prediction of the stability of a fluid layer in the atmosphere is crucial for meteorological studies. Similarly, the study of convection in the earth's mantle is important for geologists. The radiogenic heating together with thermal convection provides the driving force for any convection present in this stage of the Earth's history (see for example Tozer [3]). Nuclear fusion reaction causes volumetric heat generation in stellar interiors. The study of convection in the stars helps in obtaining information about the history of stars and various other astronomical events (Bodenschatz et al. [4]). The study of stability in a confined fluid too has a lot of applications. The heat transfer rate in the confined fluid can be increased by inducing flow. The cooling of the forward section of missiles and reentry vehicles are enhanced by induced flow. Stability analysis also finds applications in atomic power plants where a high rate of heat transfer in confined fluids is required.

A large number of investigations have been carried out on natural convection heat transfer that occurs in an enclosure due to a temperature difference across the enclosure. Most of the early investigations of this problem were based on the classical Rayleigh Benard convection that occurs in a fluid layer which is confined between two thermally conducting plates, and is heated from below to produce a fixed temperature difference (Fig. 1). Rayleigh Benard convection was first studied analytically by Lord Rayleigh in 1916 in relation to the experiments made by Benard in 1900 [5].

The present study is concerned with determining the stability of Rayleigh Benard convection with internal heat generation. Several well established methods are available in literature to determine the critical Rayleigh number for the onset of convection. The simplest approach is to numerically simulate the convection in the steady state starting with a Rayleigh number range across which the transition occurs, and using a bisection algorithm to detect the critical Rayleigh number. The onset of convection is obtained by observing the temperature contours. In the conduction regime, the temperature profiles are linear, while nonlinear temperature profiles are obtained for convection. Xia and Murthy [6] used this approach to investigate the flow transitions in deep three dimensional cavities heated from below, a configuration similar to the

* Corresponding author.
E-mail address: balaji@iitm.ac.in (C. Balaji).

0017-9310/$ - see front matter © 2009 Elsevier Ltd. All rights reserved.
doi:10.1016/j.ijheatmasstransfer.2009.04.006

Nomenclature

AR	aspect ratio of cavity, L/H
C_p	specific heat of fluid, J/kgK
g	acceleration due to gravitational, 9.8 m/s^2
H	characteristic height of the domain, m
$\hat{i}$	unit vector in x direction
$\hat{j}$	unit vector in y direction
$\hat{k}$	unit vector in z direction
K	wave number
k	thermal conductivity, W/m K
L	characteristic length of the domain, m
Nu	Nusselt number, $\frac{q_w}{(T_{\max}-T_w)}\frac{H}{k}$
Pr	Prandtl number of fluid (air), ν/α
Ra	external Rayleigh number, $\frac{g\beta\Delta TH^3}{\upsilon\alpha}$
Ra_i	internal Rayleigh number, $\frac{g\beta q''' H^5}{64\upsilon\alpha k}$
Ra^*	nondimensional heat generation, $64Ra_i$
q'''	heat generation per unit volume, W/m^3
s	growth rate
t	time, s
T	temperature of fluid, K
T_C	temperature of top plate, K
T_H	temperature of bottom plate, K
T_o	reference temperature, K
T_i	dimensionless temperature difference $\frac{k\Delta T}{q''' H^2}$
U	velocity vector
u	velocity in x direction, m/s
v	velocity in y direction, m/s
w	velocity in z direction, m/s
W	amplitude of velocity perturbation in the z direction, m/s

Greek symbols

α	thermal diffusivity, m^2/s
β	coefficient of thermal expansion, 1/K
δ_{ij}	Kronecker's delta
Θ	amplitude of temperature perturbation
κ	wavenumber in x direction
λ	wavenumber in y direction
ν	kinematic viscosity, m^2/s
ρ	density of fluid, kg/m^3
ρ_o	density of fluid at reference temperature, kg/m^3

Rayleigh Benard convection. Here, the critical Rayleigh number for the onset of convection and the transition to turbulence were studied in tall cavities.

An extrapolation of the correlation between Nusselt number and Rayleigh number obtained either using experiments or numerical simulations to the conduction value of Nusselt number also yields the critical Rayleigh number for the onset of convection. This method gives a crude approximation and can be used only for one parameter problems. Kulacki and Goldstein [7] studied, experimentally, thermal convection in a horizontal fluid layer with uniform volumetric energy sources and the results were extrapolated to obtain the critical Rayleigh number for the onset of convection.

Linear stability analysis is another method dealt with in good detail in literature ([8,9]). In linear stability analysis, the effects of small disturbances on the system are studied. The system is said to be stable if the disturbances die out in time. The nonlinear terms in the governing equations are neglected as they are insignificant during the onset. The linearized conservation equations for the disturbance quantities are solved using suitable numerical techniques to determine the critical Rayleigh number for the onset of convection. Pellew and Southwell [10] were the first to present a rigorous proof for the principle of exchange of stability. The critical Rayleigh number for the onset of Rayleigh Benard convection was established as 1708 for the rigid–rigid configuration. Ostrach and Pnueli [11] describe a method to obtain upper bounds to the instability criterion for some particular configurations. Roberts [12] carried out a linear stability analysis for the onset of convection in a horizontal fluid layer with the bottom and top plates at the same temperature and with only internal heat generation driving the convection. Tasaka and Takeda [13] studied the effects of internal heat generation with bottom wall heating on natural convection in cavities using linear stability analysis.

If the disturbances are of sufficient magnitude, the nonlinear terms in the disturbance quantities must be retained in the conservation equation describing the altered fluid motion. The deduction of the critical Rayleigh number based on the complete nonlinear equations is known as energy theory [14] and will give a stability criterion which is usually more restrictive than that of the linear theory. Fusegi et al. [15] considered a square cavity with differentially heated walls, along with volumetric heat generation, using numerical methods. They defined two Rayleigh numbers: one based on the temperature difference between the walls, and the other based on heat sources in the cavity. The basic interest of the study was to determine the effect of these Rayleigh numbers on the flow field.

From the review of literature presented above, it is seen that Rayleigh Benard convection and its applications have been extensively documented. The fundamental principles required for linear stability analysis of Rayleigh Benard convection are also well established. Numerical and experimental studies on convection in a fluid layer with only internal heat generation are also available in literature. The linear stability analysis for the onset of convection in fluid layer with internal heat generation has also been discussed in literature. Even so, scarce are studies that address the effect of internal heat generation on the onset of Rayleigh Benard convection in spite of its potential applications in several problems in science and engi-

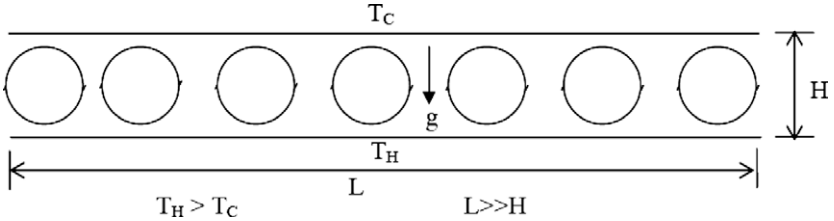

Fig. 1. Schematic of Rayleigh Benard convection.

neering. Furthermore, from a fundamental standpoint, it would be interesting to see at what aspect ratio, the cavity starts behaving like an infinite cavity for which a simple linear stability analysis to determine the onset of convection would suffice.

2. Methodology

The geometry and the boundary conditions for the problem under consideration are shown in Fig. 2. The bottom and top plates are isothermal with the bottom plate at a higher temperature and the side walls are adiabatic. The fluid layer is given a uniform volumetric internal heat generation. The aspect ratio of the cavity is defined as the ratio of the horizontal dimension to the vertical dimension. The cavity is infinitely deep in the plane perpendicular to the paper.

2.1. Methodology for linear stability analysis

The onset of convection is studied analytically using linear stability analysis for an infinitely wide cavity. The behavior of the system for a given perturbation is studied to determine the stability of the system. The equations of the system in the perturbed state are obtained as given below. The terms involving the products of perturbations are neglected.

$$\nabla \cdot u' = 0 \tag{1}$$

$$\frac{\partial u'}{\partial t} = -\frac{\nabla P'}{\rho_0} + \nu\nabla^2 u' + g\beta T' \tag{2}$$

$$\frac{\partial T'}{\partial t} + u' \cdot \nabla \overline{T} = \alpha\nabla^2 T' \tag{3}$$

The above equations are made dimensionless and are manipulated to obtain the perturbation equation. Here, the domain is infinite in the x and y directions making the problem essentially one dimensional in the z direction

$$\nabla \cdot \tilde{w}' = 0 \tag{4}$$

$$\frac{\partial}{\partial \tilde{t}}(\nabla^2 \tilde{w}') = Ra^* \mathrm{Pr}\nabla_H^2 \theta' + \mathrm{Pr}\nabla^4 \tilde{w}' \tag{5}$$

here $Ra^* = 64Ra_i$

$$\frac{\partial \theta'}{\partial \tilde{t}} + w' \frac{\partial \theta'}{\partial \tilde{z}} = \nabla^2 \theta' \tag{6}$$

Eliminating θ', the perturbation equation in $\tilde{w}'$ is obtained as given below

$$\left(\frac{\partial}{\partial \tilde{t}}\nabla^2 - \mathrm{Pr}\nabla^4\right)\left(\frac{\partial}{\partial \tilde{t}} - \nabla^2\right)\tilde{w}' = -\frac{\partial \theta}{\partial \tilde{z}} Ra^* \mathrm{Pr}\nabla_H^2 \tilde{w}' \tag{7}$$

The above expression gives the perturbation equation in $\tilde{w}'$. The perturbations given are of the form as given below,

$$\tilde{w}' = We^{i(\kappa x + \lambda y) + st} \quad \text{and} \quad \theta' = \Theta e^{i(\kappa x + \lambda y) + st} \tag{8}$$

Substituting the perturbation in Eq. (7) and simplifying, a sixth order ordinary differential equation is obtained.

$$(D^2 - K^2)(D^2 - K^2 - s)\left(D^2 - K^2 - \frac{s}{\mathrm{Pr}}\right)W = Ra^* K^2 WD\bar{\theta} \tag{9}$$

In the above equation D is the differential operator $D = \frac{\partial}{\partial z}$ and $K = \sqrt{\kappa^2 + \lambda^2}$ is the wave number. Following [8], "s" is real for all positive Rayleigh numbers (i.e. for all adverse temperature gradients); it follows that the transition from stability to instability must occur via a stationary state. The equation governing the marginal stability is obtained by setting $s = 0$ in the above equation.

$$(D^2 - K^2)^3 W = Ra^* K^2 WD\bar{\theta} \tag{10}$$

$D\bar{\theta}$ is obtained from the temperature profile in the base $(\bar{\theta})$ state, by solving the energy equation with boundary conditions.

When the bottom plate is at higher temperature compared to the top plate,

$$D\bar{\theta} = \left(\frac{1}{2} - T_i - \tilde{z}\right) \tag{11}$$

When the top plate is at higher temperature compared to the bottom plate,

$$D\bar{\theta} = \left(\frac{1}{2} + T_i - \tilde{z}\right) \tag{12}$$

$$\text{Where } T_i = \frac{k\Delta T}{q''' H^2} \tag{13}$$

2.1.1. Boundary conditions

The equation to be solved is a sixth order differential equation and hence requires six boundary conditions. Here, both the boundaries considered are rigid. For the rigid–rigid configuration, the boundary conditions are as explained below:

The fluid is confined between two planes which are maintained at constant temperature giving $\theta' = 0$ and $\tilde{w} = 0$ for $\tilde{z} = 0$, and 1.

The no-slip condition on a rigid boundary $\tilde{z} = 0$ and $\tilde{z} = 1$ implies $\tilde{u} = \tilde{v} = \tilde{w} = 0$, at both the boundaries and hence it follows from the equation of continuity equation that $\frac{\partial \tilde{w}}{\partial \tilde{z}} = 0$.

Using the boundary condition $\theta' = 0$ we obtain

$$(D^2 - K^2)\left(D^2 - K^2 - \frac{s}{\mathrm{Pr}}\right)W = 0 \tag{14}$$

The six boundary conditions for the problem in the case of marginal stability analysis i.e. $s = 0$ are as given,

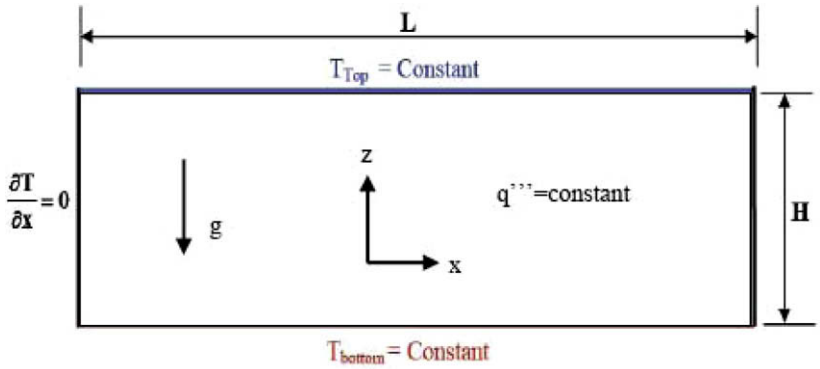

Fig. 2. Problem geometry and boundary conditions.

$$W = DW = (D^2 - K^2)^2 W = 0 \quad \text{at } \tilde{z} = 0, 1 \tag{15}$$

In Eq. (10), only for a particular value of Ra^* for a given K^2 will the problem allow non zero solutions. Thus, the problem is a characteristic value problem for Ra^*. For a given K^2, the lowest characteristic value for Ra^* is to be determined, the minimum of all the Ra^* thus obtained is the critical Ra^* at which the instability manifests itself.

2.1.2. Solution scheme

The shooting method is used for solving the sixth order differential eigen value problem given in Eq. (10) for a particular K. The details of the method are presented in Chapra and Canale [16]. The solution of six first order equations requires six initial conditions and an extra equation for Ra^*. The extra equation for Ra^* is obtained from the fact that Ra^* is independent of $\tilde{z}$

$$\frac{\partial Ra^*}{\partial \tilde{z}} = 0 \tag{16}$$

A fourth order Runge Kutta scheme is used to integrate the equations from $\tilde{z} = 0$ to $\tilde{z} = 1$. Three of the six end conditions are known at the boundary $\tilde{z} = 1$. The end conditions are checked and the initial guess for the boundary conditions and value of Ra^* are corrected using the Newton Raphson method of solving non-linear simultaneous equations until convergence is obtained within permissible error.

The above procedure is repeated for other values of K and one can obtain a plot of Ra^* v/s K and the minimum value of Ra^* gives the critical Ra^* for that particular T_i. The procedure is repeated for various values of T_i to obtain the stability curve of Rayleigh Benard convection with internal heat generation of an infinite aspect ratio. To be consistent with literature, plots of Ra_i v/s K are drawn using the relation $Ra^* = 64Ra_i$.

2.2. Methodology for the "full" numerical (CFD) analysis

Convection in a fluid layer heated from below and with internal heat generation is analyzed numerically using the commercially available FLUENT 6.3. The bottom and top plate are isothermal and the side walls are adiabatic. The fluid layer is given a uniform volumetric internal heat generation. The Boussinesq approximation is assumed to hold good. For the above conditions, the governing equations for mass, momentum and energy for a steady, 2-D, laminar, incompressible flow with the Boussinesq approximation are

$$\frac{\partial u}{\partial x} + \frac{\partial w}{\partial z} = 0 \tag{17}$$

$$u\frac{\partial u}{\partial x} + w\frac{\partial u}{\partial z} = -\frac{1}{\rho_0}\frac{\partial P}{\partial x} + \nu\nabla^2 u \tag{18}$$

$$u\frac{\partial w}{\partial x} + w\frac{\partial w}{\partial z} = -\frac{1}{\rho_0}\frac{\partial P}{\partial z} + \nu\nabla^2 w + g\beta(T - T_0) \tag{19}$$

$$u\frac{\partial T}{\partial x} + w\frac{\partial T}{\partial z} = \alpha\nabla^2 T + \frac{q'''}{\rho_0 C_p} \tag{20}$$

2.2.1. Solution scheme

First a suitable grid pattern is chosen and meshing is done. All properties are calculated at the mean temperature and Boussinesq approximation is used for modeling the natural convection flow. The bottom and top wall are given isothermal boundary conditions, the side walls are kept adiabatic and a uniform internal heat generation is given as a source term in the fluid zone. The SIMPLE algorithm is used for the pressure velocity coupling. A first order upwind scheme is used for both the momentum and energy equations. The solution is considered converged if the residuals for the continuity, x and y momentum equations are less than 1×10^{-8} and less than1×10^{-10} for the energy equation.

The shape of the temperature contours is used to determine the onset of convection. When Ra is lower than Ra_c (i.e. critical Rayleigh number), the temperature contours are parallel to the horizontal dimension. For $Ra > Ra_c$, the temperature contours depart from the linear profile quite substantially. Thus, the Rayleigh number was changed in small steps by changing the temperature difference or by changing the internal heat generation until convection is observed. To obtain accurate results, the bisection algorithm is used to improve the guess. The above method is used to predict the Ra_c with an accuracy of ±10.

The problem is basically a two parameter one with the two parameters being Ra and Ra_i (the Rayleigh number based on temperature difference and internal heat generation, respectively). The objective of the study is to determine the critical values of the pair (Ra, Ra_i) for which the onset of convection occurs. Here, for each aspect ratio, the critical Ra (Ra_{cr}) is determined by keeping Ra_i constant and vice versa. While infinite combinations of Ra and Ra_i are possible for each aspect ratio, due to computational limitations, we limit our study to obtain five sets of critical values of the pair (Ra, Ra_i) for each aspect ratio. Two sets of Ra_c are obtained at $Ra = 0$ and $Ra_i = 0$ by varying Ra_i and Ra, respectively, and the other three were obtained by keeping Ra as constant and by varying the internal heat generation. The study was done for eight different aspect ratios 1, 2, 3, 4, 5, 6, 8 and 10. A total of 40 pairs of Ra_c were thus obtained. The important non dimensional numbers in the study are (1) Rayleigh number, Ra given by $\frac{g\beta\Delta TH^3}{\upsilon\alpha}$ and (2) the internal Rayleigh number, Ra_i given by $\frac{g\beta q''' H^5}{64\upsilon\alpha k}$.

3. Validation

3.1. Validation of the linear stability analysis code

The Rayleigh number for the onset of convection in Rayleigh Benard convection is available in literature, as a number of experimental and analytical studies have already been done as already mentioned. Here, the onset of convection between two infinite parallel plates at a constant temperature with the bottom plate at a higher temperature compared to the top plate is studied. The linear stability code developed for this study was first validated using the onset of convection for Rayleigh Benard convection. The equation to be solved and the boundary conditions are given in Eqs. (10)

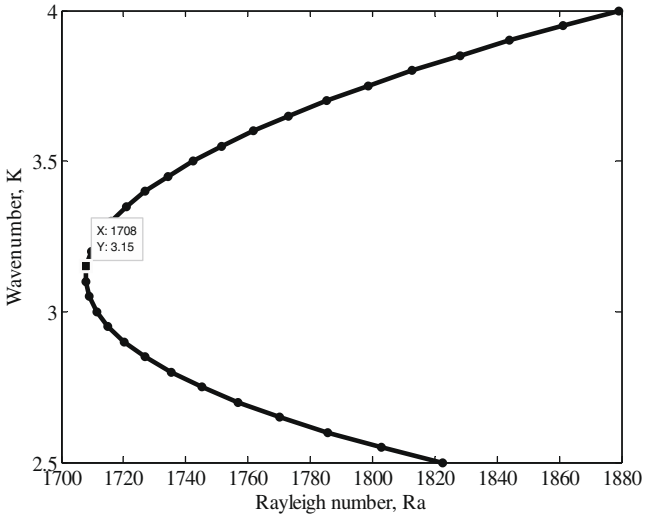

Fig. 3. Stability plot for Rayleigh Benard convection without internal heat generation.

and (15), respectively. The stability plot for Rayleigh Benard convection is given in Fig. 3.

The critical Rayleigh number for Rayleigh Benard convection is obtained as 1708 using linear stability analysis and the value exactly matches with the values available in the literature see, for example Pellew and Southwell [10]. The code is also validated for case of convection with only heat generation. In this configuration, the two infinitely long parallel isothermal plates are kept at the same temperature. The confined fluid is given a uniform internal heat generation. The Ra_i obtained from linear stability analysis is 583.1, as shown in the Fig. 4. The results again match very well with the values reported by Kulacki et al. [14]. Thus, the formulation and the code for linear stability analysis were found to be working satisfactorily. The code is now used to obtain the onset of convection for cases in which both temperature difference and internal heat generation act together as driving forces.

3.2. Validation of the full numerical (CFD) model

To validate the model, the results of the present study for thermal convection in a horizontal fluid layer with internal heat generation are compared with experimental results available in literature. The details of the experimental study by Kulacki and Goldstein [7] on thermal convection in a horizontal fluid layer with uniform volumetric heat generation are shown in Fig. 5. Joule heating by an alternating current passing horizontally through the layer produced the required volumetric heat generation. Experiments were conducted in the Rayleigh number (Ra_i), range 196–10^5, where Ra_i is defined as $\frac{g\beta H^5 q'''}{64\alpha\nu k}$. Kulacki and Goldstein developed two correlations for the Nusselt number given by,

$$Nu = 0.879\mathrm{Ra}^{0.236} \quad \text{for the upper plate} \tag{21}$$

$$Nu = 2.11\mathrm{Ra}^{0.094} \quad \text{for the lower plate} \tag{22}$$

In the present study, simulations are carried out by varying the Rayleigh number in the range 1500–378500. The bottom and top plates are given a uniform temperature of 300 K and the side walls are maintained adiabatic. A uniform internal heat generation is given in the fluid domain. No-slip conditions are imposed on all the walls. A plot of the average Nusselt number with the Rayleigh number is given in Fig. 6.

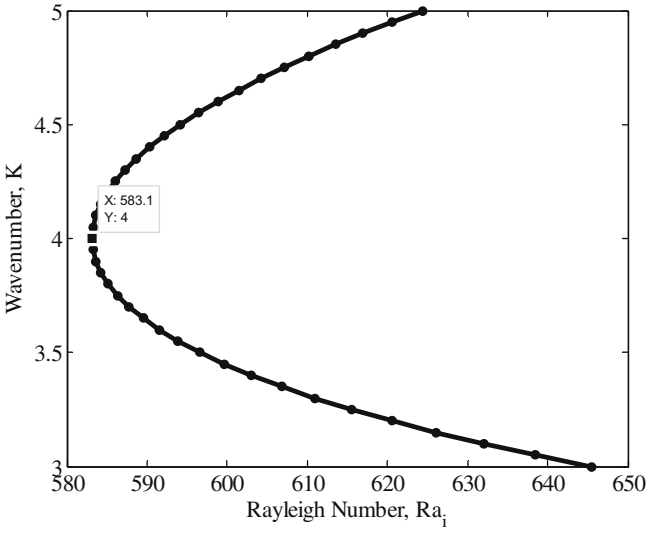

Fig. 4. Results for the onset of convection in a cavity with only internal heat generation.

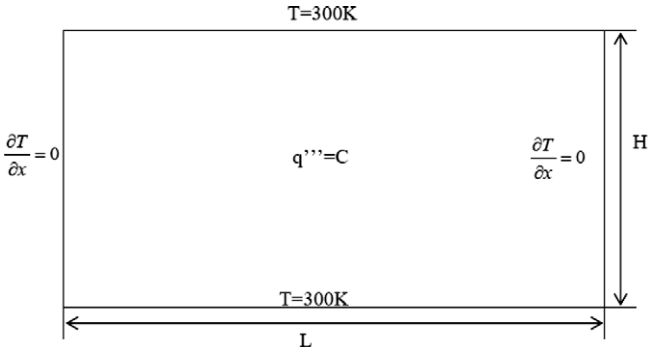

Fig. 5. Schematic of the experimental setup used by Kulacki and Goldstein [7].

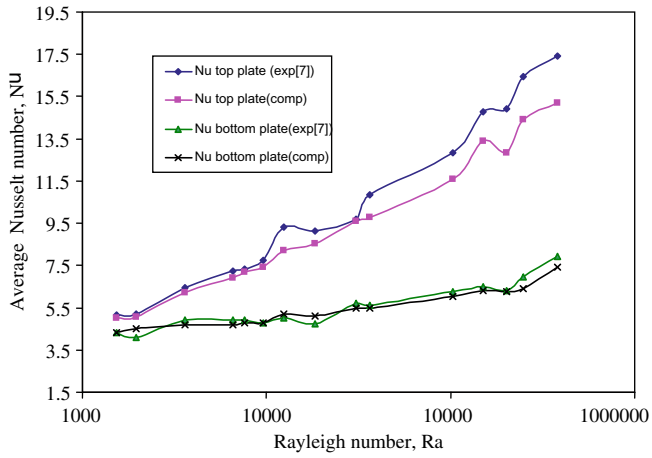

Fig. 6. Variation of average Nusselt number with Rayleigh number for the top and bottom plates.

The values of the average Nusselt number from the numerical simulations are found to match the experimental observations of [7] very well, with the average error being less than 10%. It is seen that when the Rayleigh number is increased, the Nusselt number at the top plate is almost twice that in the bottom plate. The fraction of energy transported to the upper boundary (F_H) is defined as $F_H = \frac{Nu_{top}}{Nu_{top}+Nu_{bottom}}$, and the results are shown in Fig. 7. It is found that above a Rayleigh number of 10^5, about 70% of the internal heat generated is transported to the upper wall.

The spatially averaged temperature distribution (averaged in the horizontal dimension of the cavity) is shown in Fig. 8. A number of distinct features of low and high Rayleigh number convection are identifiable from the temperature profiles. For Rayleigh numbers less than 600, the mode of heat transfer is only conduction and the temperature profile is parabolic and symmetric about the mid plane. When the Rayleigh number is increased further, the temperature profile becomes asymmetric as convection sets in. In general, at higher Rayleigh numbers the overall buoyancy force acting on the warm central core of the fluid layer displaces this region upwards and above the geometric centre of the layer, making the overall temperature profile asymmetric. The asymmetric nature of the temperature profile further increases, as the Rayleigh number is increased.

The slope of the temperature profile near the top wall is almost twice the slope near the bottom wall, thus corroborating our earlier findings that the energy transported to the top wall is almost twice the energy transported to the bottom wall. It is found that, in general, CFD simulations match the experimental observation quite satisfactorily. A parabolic temperature profile is obtained in

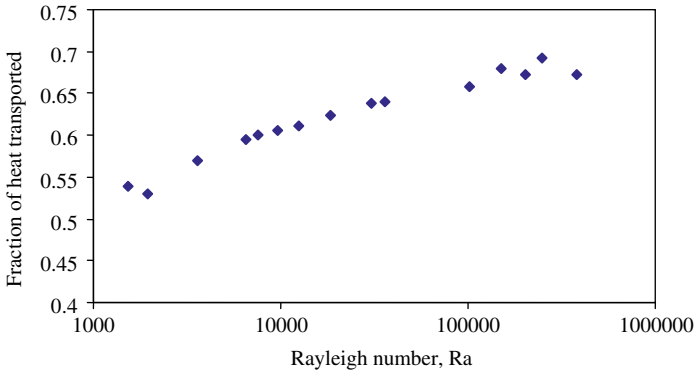

Fig. 7. Fraction of energy transported to the upper boundary.

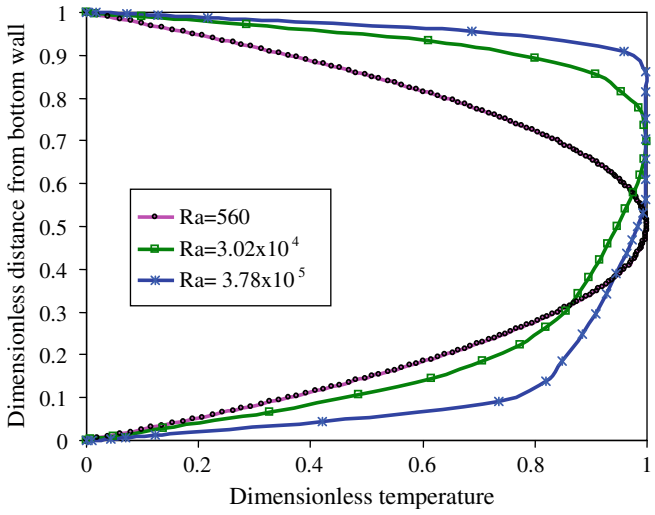

Fig. 8. Variation of temperature across the cavity for various Rayleigh numbers.

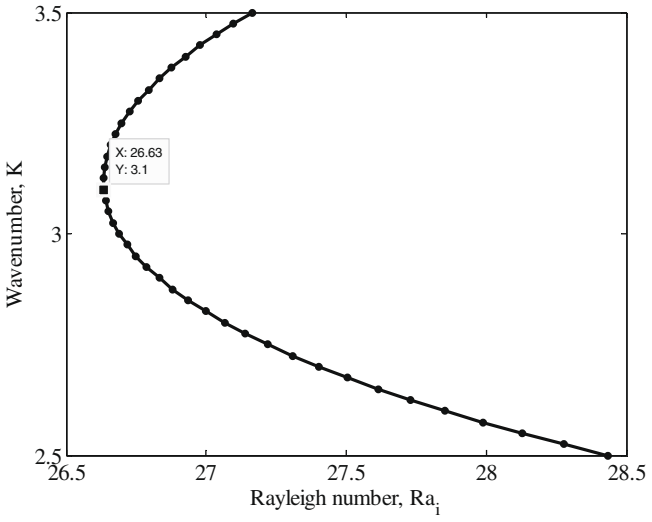

Fig. 9. Stability curve for $T_i = 1$.

the conduction regime, which is expected for heat transfer in a fluid layer with internal heat generation. The contours of temperature are parallel to the horizontal dimension in the conduction regime but rolls starts to form as convection set in. Thus, the onset of convection can be studied by observing the temperature contours obtained directly from steady state simulations.

4. Results and discussion

4.1. Linear stability analysis

In the present study, the critical Rayleigh numbers are calculated by solving the sixth order differential equation described in Eq. (10), for different values of T_i using the shooting method. The calculations are done for T_i varying from 0 to 1000. Here, the bottom plate is kept at a higher temperature compared to the top plate and this resembles the classical Rayleigh Benard convection. Fig. 9 shows a plot of Ra^* versus K for $T_i = 1$ as an example. The principle of exchange of stability is assumed to hold good and so here the marginal stability analysis is carried out at $s = 0$, as already mentioned. The stability curve for Rayleigh Benard convection ($T_i = \infty$) and convection in fluid layer with only heat generation ($T_i = 0$) were already discussed (Figs. 3 and 4). The results obtained from the stability analysis are in terms of Ra_i and T_i, while the CFD results are in the terms of Ra and Ra_i. To facilitate comparison with CFD results, the analytical results are recalculated in terms of Ra and Ra_i and are given in Table 1.

Table 1
Onset study using linear stability analysis.

Sl No.	T_i	K	Ra_i	Ra
1	0	4	583.1	0
2	0.01	3.9	524.3	335.5
3	0.02	3.8	472.1	604.288
4	0.04	3.6	385.1	985.856
5	0.06	3.45	318.3	1222.272
6	0.08	3.4	267.5	1369.6
7	0.1	3.3	228.6	1463.04
8	0.2	3.2	127.6	1633.28
9	0.4	3.15	65.94	1688.064
10	1	3.1	26.63	1704.32
11	10	3.1	2.668	1707.52
12	100	3.1	0.2668	1707.63
13	1000	3.1	0.02668	1707.75
14	RBC[a]	3.1	0	1708

[a] RBC, Rayleigh Benard convection.

The stability curve for an infinitely long cavity obtained from the linear stability analysis is presented in Fig. 10. The region in the plot below the curve is stable with only conduction; convection is present for regions above the curve. From the study, it is clear that internal heat generation aids the onset of convection. The curve is highly steep near $Ra = 1708$, the critical value for the onset of Rayleigh Benard convection. It is clear that for very high Ra, heat generation plays an insignificant role on the onset and the effect of internal heat generation is more pronounced for low Ra (external Rayleigh number).

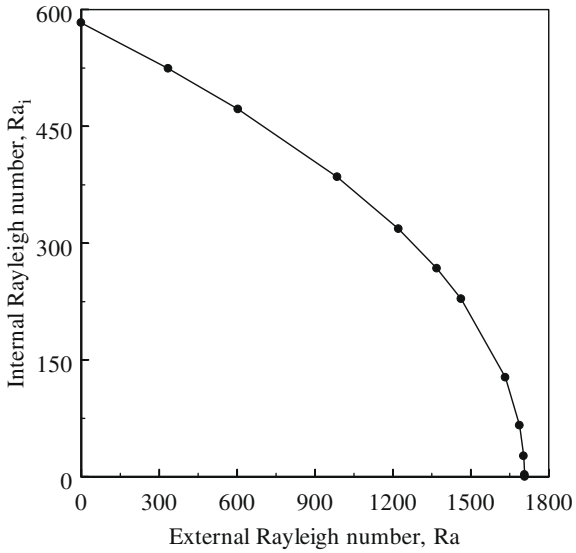

Fig. 10. Stability curve for an infinitely long cavity with the bottom plate at a higher temperature.

For the problem under consideration the equation of the stability curve is derived to be

$$\frac{Ra}{1708} + \left(\frac{\mathrm{Ra}_i}{583.1}\right)^2 - 1 = 0 \tag{23}$$

The above equation can be used to determine the onset of Rayleigh Benard convection for an infinitely wide horizontal cavity with heat generation. The fluid layer will have only conduction for all pairs of Ra and Ra_i for which $\frac{Ra}{1708} + \left(\frac{Ra_i}{583.1}\right)^2 \leq 1$, else there will be convection in the fluid layer. The parity plot obtained for Ra_{cr} and Ra_{icr} obtained using the above equation is shown in Fig. 11.

4.2. Results of full numerical simulations (CFD)

4.2.1. Grid independence study

A grid independence study has been carried out for an aspect ratio of 10 which is the worst case possible from the point of view of grid dependence. The Rayleigh number for the simulation was selected as (Ra = 3800). The geometry and the boundary conditions

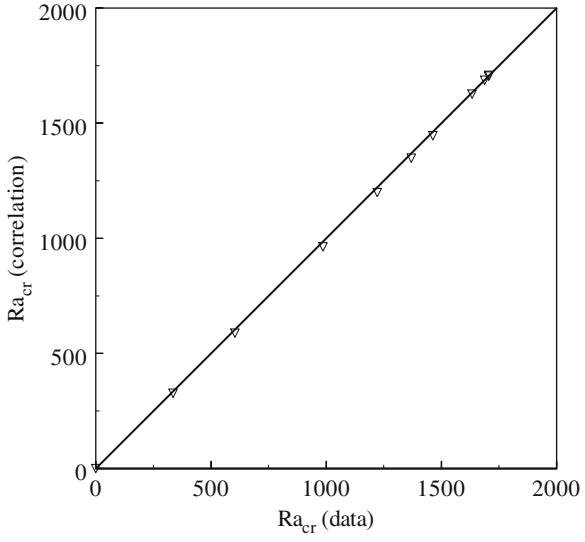

Fig. 11. Parity plot highlighting the goodness of fit of Eq. (23).

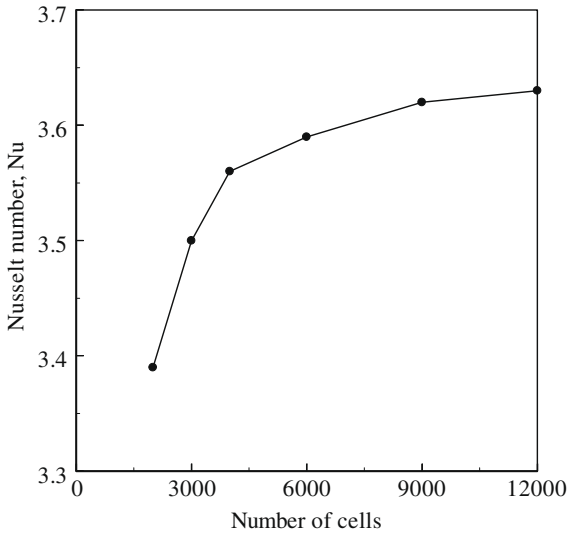

Fig. 12. Results of the grid independence study for AR = 10 and Ra = 3800.

are given in Fig. 2. The average Nusselt number obtained for various grid patterns are shown in Fig. 12. The difference in the average Nusselt number obtained using 12000 cells and with that obtained by using 9000 cells is less than 0.5%. Here, a grid with 9000 cells with uniform spacing in the x and z directions is selected for further simulations.

4.2.2. Onset of convection for various aspect ratios

Numerical simulations are carried out for laminar Rayleigh Benard convection with internal heat generation spanning eight different aspect ratios (1, 2, 3, 4, 5, 6, 8, and 10) to obtain the critical Rayleigh number for the onset of convection. The onset of convection is studied primarily by observing the temperature contours obtained from steady state simulations, as already discussed. For each aspect ratio, five pairs of (Ra, Ra_i) are obtained. Each pair of (Ra, Ra_i) is obtained by running steady state simulations starting with the Rayleigh number range across which transition occurs and using the bisection algorithm to detect the critical Rayleigh numbers by observing the temperature contours. It is also observed that during the onset of convection, the magnitude of velocity is higher by an order of magnitude and rolls are present in the fluid layer compared to a fluid layer with only conduction. Roughly three hundred simulations were carried out to obtain 40 pairs of (Ra, Ra_i). The results of the stability analysis for (i) Rayleigh Benard convection (ii) convection in a fluid layer with only heat generation and (iii) Rayleigh Benard convection with internal heat generation are discussed below. The main focus of the CFD analysis here is the effect of aspect ratio on the onset of convection.

4.2.2.1. Stability analysis for "plain" Rayleigh Benard convection. The critical Rayleigh number for the onset of convection is obtained by examining the temperature contours. The effect of aspect ratio on the onset of convection is given in Fig. 13. The critical Rayleigh number approaches the value of 1708 as the aspect ratio is increased beyond 8 confirming with the values available in literature. The critical Ra decreases with the increase in aspect ratio as the effect of side wall effect becomes less significant at higher aspect ratios. In general, the side wall creates a resistance to the convection flow as boundary layers are formed near the side walls. The no-slip condition near the side wall causes hindrance to the flow and the viscous forces increase resulting in a higher critical Rayleigh number for the onset of convection. It is clear from the study that the effects of side wall are negligible as the aspect ratio is increased beyond 8.

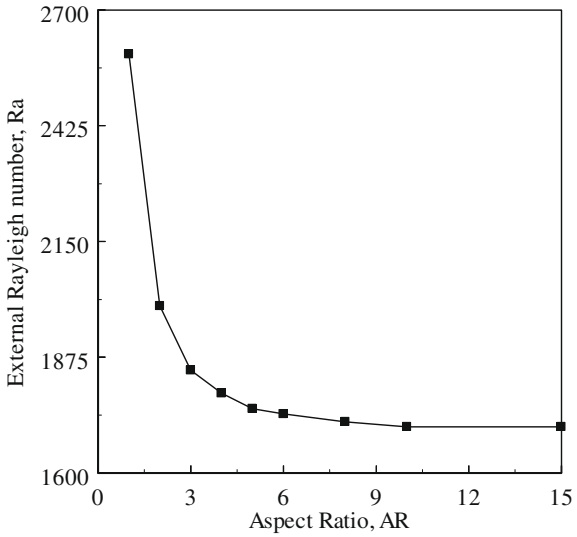

Fig. 13. Effect of aspect ratio on the onset of Rayleigh Benard convection.

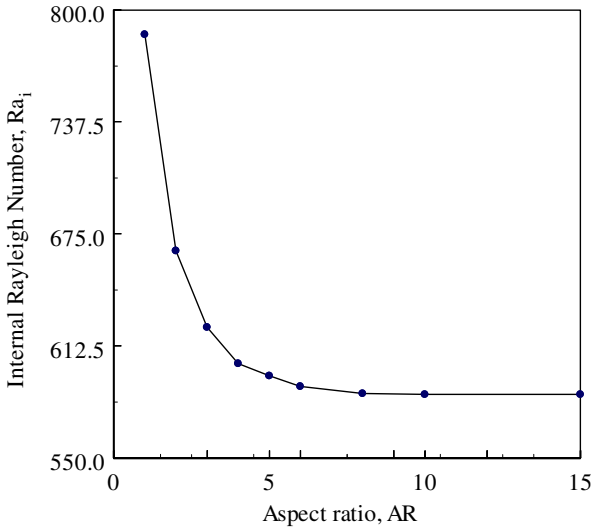

Fig. 15. Effect of aspect ratio on the onset of convection in a cavity with only internal heat generation.

The correlation for critical Rayleigh number for aspect ratios (AR) varying from 1 to 15 is obtained from the study using regression

$$\frac{Ra_{cr}}{1708} = \frac{0.469}{AR^2} + \frac{0.0627}{AR} + 1 \tag{24}$$

Here Ra_{cr} is the critical external Rayleigh number for the onset of convection for Rayleigh Benard convection. The form of the above equation is so chosen that Ra_{cr} tends to 1708 as AR $\to \infty$. Eq. (24) has an R^2 value of 0.99 and an RMS error of ±6.24. A parity plot demonstrating the goodness of the fit can be seen in Fig. 14.

4.2.2.2. Stability analysis for convection in fluid layers with only heat generation. The critical Rayleigh number (Ra_i) varies from 756 for an aspect ratio of 1 to 563 for an aspect ratio of 10. The variation of Ra_i with aspect ratio is shown in Fig. 15. The trend shown is similar to that seen for the "plain" Rayleigh Benard convection. The side walls have a noticeable effect for small aspect ratios. However, this becomes imperceptible above an aspect ratio of 8. The critical Ra_i obtained for aspect ratio of 10 agrees well with the results of the analytical study, where a cavity of infinite aspect ratio is considered. A correlation for the critical Rayleigh number for aspect ratios (AR) varying from 1 to 15 is obtained from the study as

$$\frac{Ra_{i_{cr}}}{583.1} = \frac{0.265}{AR^2} + \frac{0.097}{AR} + 1 \tag{25}$$

Here Ra_{icr} is the critical internal Rayleigh number for the onset of convection in a horizontal fluid layer with only heat generation with both the bottom and top plates being kept at the same temperature. Eq. (25) has a R^2 value of 0.99 and an RMS error of ±4.35. A parity plot, shown in Fig. 16 shows the excellent agreement between the data and the predictions.

4.2.2.3. Stability analysis for Rayleigh Benard convection with heat generation. The stability curves of Rayleigh Benard convection with internal heat generation for different aspect ratios are shown in Fig. 17. The region below each curve shows the stable region for that particular aspect ratio. The critical Rayleigh numbers for the

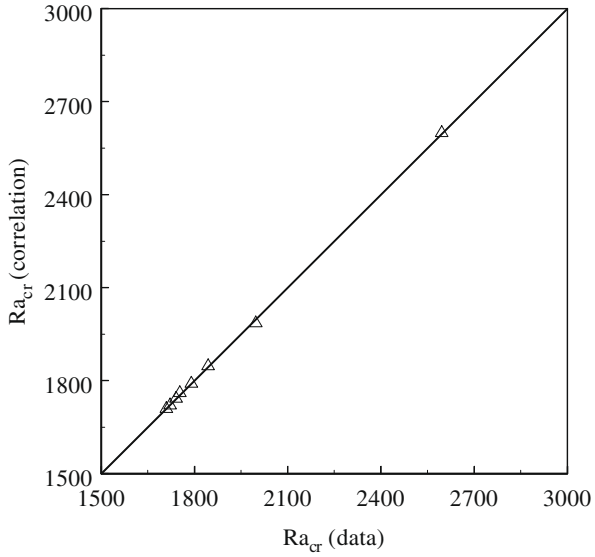

Fig. 14. Parity plot highlighting the goodness of fit of Eq. (24).

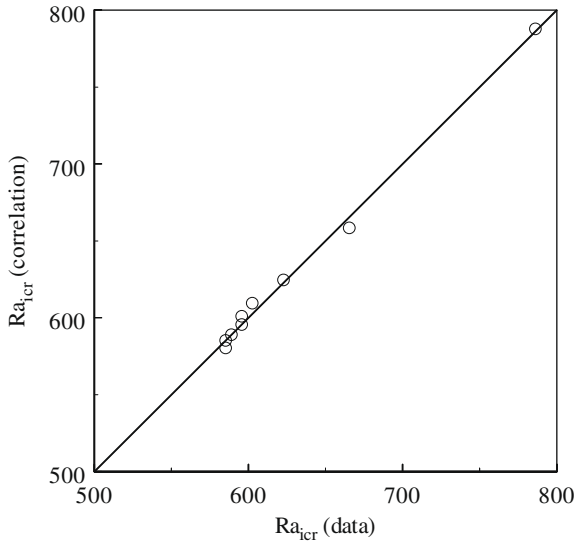

Fig. 16. Parity plot highlighting the goodness of fit of Eq. (25).

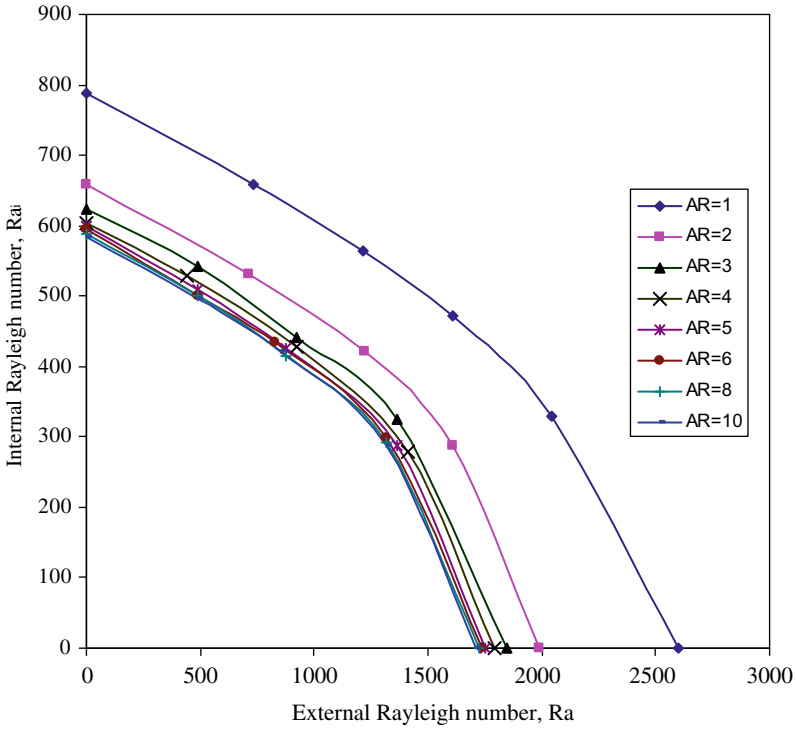

Fig. 17. Stability curves for various aspect ratios.

onset of convection decrease as the aspect ratio is increased because the effect of the side wall reduces as the aspect ratio is increased. The variation of critical Rayleigh numbers for aspect ratios 6, 8 and 10 are insignificant.

A general correlation applicable for all aspect ratios and for all the three physical scenarios considered in this paper has been developed based on 40 data spanning the range of aspect ratios varying from 1 to 10 and is given below.

$$\frac{Ra}{Ra_{cr}} + \left(\frac{Ra_i}{Ra_{icr}}\right)^2 - 1 = 0 \tag{26}$$

Where Ra_{cr} and Ra_{icr} are given by Eqs. (24) and (25), respectively. Using Eqs. (24)–(26), the stability curve for any aspect ratio varying from 1 to 10 can be obtained. The parity plot obtained for Ra_{cr} and Ra_{icr} obtained using the above equations are shown in Figs. 18 and 19, respectively. Eq. (26) reduces to Eq. (23) for the case of AR → ∞, thus corroborating its asymptotic correctness.

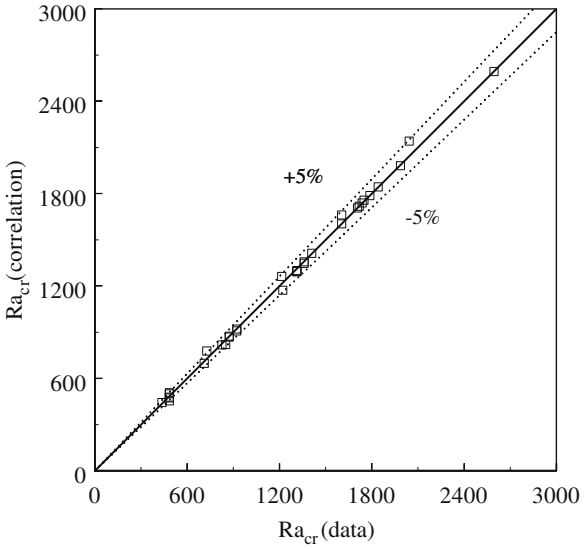

Fig. 18. Parity plot highlighting the goodness of fit of Eq. (26) for Ra_{cr}.

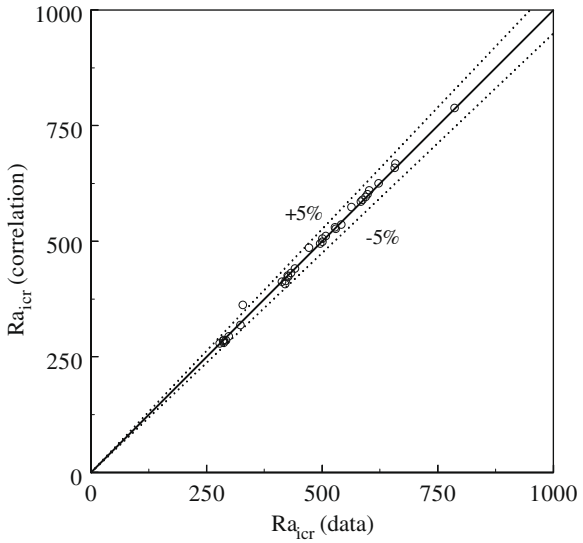

Fig. 19. Parity plot highlighting the goodness of fit of Eq. (26) for Ra_{icr}.

5. Comparison of CFD and analytical results

The stability curve for the onset of convection obtained from both CFD analysis (AR = 10) and the linear stability analysis (for infinite domain) agree very well with each other as seen in Fig. 20. The maximum difference is less than 3%. It can now be concluded that a closed cavity of aspect ratio 10 simulates two infinite parallel plates quite satisfactorily for the given problem. Therefore,

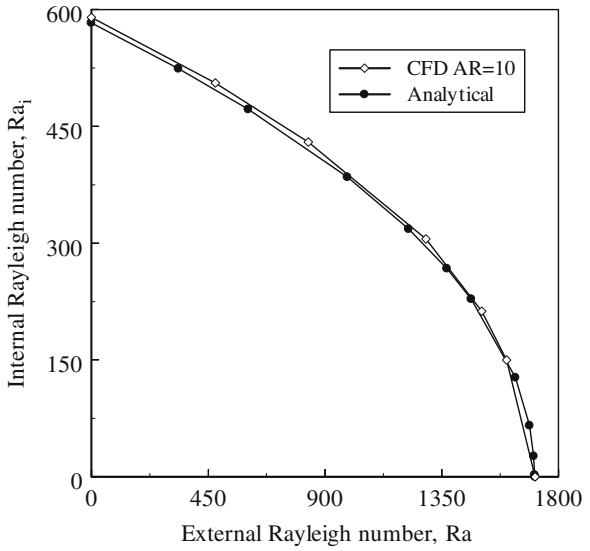

Fig. 20. Comparison of full numerical (CFD) solutions with those from the linear stability analysis.

one may choose to work on AR = 10 for conducting any further studies on laminar Rayleigh Benard convection with internal heat generation to reduce the computational effort.

6. Conclusions

Numerical investigations were carried out for two dimensional, laminar Rayleigh Benard convection, with internal heat generation spanning eight different aspect ratios, to obtain the critical Rayleigh number for the onset of convection. The onset for an infinitely long cavity was determined using linear stability analysis and the following conclusions were arrived at:

1. In general internal heat generation aids the onset of convection.
2. The critical Rayleigh number for the onset of convection decreases with the increase in aspect ratio as the influence of the side wall decreases as the aspect ratio is increased as expected.
3. From the stability curves drawn for various aspect ratios and for AR = 10, it is seen that the cavity approaches the limit of an infinite cavity at this aspect ratio, for which analytical results obtained by using linear stability analysis agree very well with the "full" CFD simulations.
4. A comprehensive yet simple correlation to determine the onset of convection when both temperature difference and volumetric heat generation are present, valid for a wide range of aspect ratios has been proposed. The asymptotic correctness of the correlation has also been verified.

References

[1] E.M. Agee, T.S. Chen, K.E. Dowell, A review of mesoscale cellular convection, Bull. Am. Meteorol. Soc. 54 (1973) 1004–1012.
[2] Jefrey Rothermel, Ernset M. Agee, A numerical study on atmospheric scaling, J. Atmos. Sci. 43 (1986) 1185–1197.
[3] D.C. Tozer, Heat transfer and convection currents, Proc. Roy. Soc. Lond. A, Math. Phys. Sci. 258 (1965) 252–270.
[4] Eberhard Bodenschatz, Werner Pesch, Guenter Ahlers, Recent Developments in Rayleigh–Benard Convection, Ann. Rev. Fluid Mech. 32 (2003) 709–778.
[5] A. Bejan, Convection Heat Transfer, John Wiley and Sons, New York, 1993.
[6] Chunmei Xia, Jayathi Y. Murthy, Buoyancy-driven flow transitions in deep cavities heated from below, ASME J. Heat Transfer 124 (2002) 650–659.
[7] F.A. Kulacki, R.J. Goldstein, Thermal convection in fluid layer with uniform volumetric energy sources, J. Fluid Mech. 55 (1972) 271–284.
[8] S. Chandrasekhar, Hydrodynamic and Hydromagnetic Stability, Clarendon Press, Oxford, 1961.
[9] P.G. Drazin, W.H. Reid, Hydrodynamic Stability, Cambridge University Press, 2004.
[10] Anne Pellew, R.V. Southwell, On maintained convective motion in a fluid heated from below, Proc. Roy. Soc. Lond. A, Math. Phys. Sci. 176 (1940) 312–343.
[11] S. Ostrach, D. Pnueli, The thermal instability of a completely confined fluids inside some particular configuration, ASME J. Heat Transfer 64 (1963) 346–352.
[12] P.H. Roberts, Convection in horizontal fluid layers with internal heat generation Theory, J. Fluid Mech. 30 (1967) 33–49.
[13] Tasaka Yuji, Takeda Yasushi, Effects of heat source distribution on natural convection induced by internal heating, Int. J. Heat Mass Transfer 48 (2005) 1164–1174.
[14] F.A. Kulacki, R.J. Goldstein, Hydrodynamic instability in fluid layers with uniform volumetric energy sources, Appl. Sci. Res. 31 (1975) 81–109.
[15] T. Fusegi, J.M. Hyun, K. Kuwara, Natural Convection in a Differentially Heated Cavity With Internal Heat Generation, Numer. Heat Transfer A 21 (1992) 215–229.
[16] Chapra Steven, Canale Raymond, Numerical Methods for Engineers, Mc Graw Hill, New York, 2006.